IOP PUBLISHING PHYSICS IN MEDICINE AND BIOLOGY

Phys. Med. Biol. **52** (2007) 5945–5955 doi:10.1088/0031-9155/52/19/015

Monte Carlo simulation of a computed tomography x-ray tube

Magdalena Bazalova and Frank Verhaegen

Medical Physics Department, McGill University, Montreal General Hospital, 1650 Cedar Avenue, Montreal, Québec H3G1A4, Canada

E-mail: fverhaegen@medphys.mcgill.ca

Received 6 July 2007, in final form 22 August 2007
Published 17 September 2007
Online at stacks.iop.org/PMB/52/5945

Abstract

The dose delivered to patients during computed tomography (CT) exams has increased in the past decade. With the increasing complexity of CT examinations, measurement of the dose becomes more difficult and more important. In some cases, the standard methods, such as measurement of the computed tomography dose index (CTDI), are currently under question. One approach to determine the dose from CT exams is to use Monte Carlo (MC) methods. Since the patient geometry can be included in the model, Monte Carlo simulations are potentially the most accurate method of determining the dose delivered to patients. In this work, we developed a MC model of a CT x-ray tube. The model was validated with half-value layer (HVL) measurements and spectral measurements with a high resolution Schottky CdTe spectrometer. First and second HVL for beams without additional filtration calculated from the MC modelled spectra and determined from attenuation measurements differ by less than 2.5%. The differences between the first and second HVL for both filtered and non-filtered beams calculated from the MC modelled spectra and spectral measurements with the CdTe detector were less than 1.8%. The MC modelled spectra match the directly measured spectra. This works presents a first step towards an accurate MC model of a CT scanner.

(Some figures in this article are in colour only in the electronic version)

1. Introduction

Computed tomography (CT) is an essential part of today's radiological diagnostics. CT is a high performance imaging modality that combines good image resolution with high tissue contrast. Due to the advances in CT technology, the relative number of CT examinations of all radiological examinations has increased from 2% to 10–15% in some countries in the past ten years (Rehani *et al* 2001). As a result, their contribution to the total dose from medical examinations is very significant, accounting for 34% of the collective dose

(Rehani *et al* 2001). Epidemiological studies have shown that the absorbed dose to tissues from CT can often approach or exceed levels known to increase the probability of cancer (Rehani *et al* 2001).

With the development of new CT techniques, such as multi-slice CT, cine CT or cone beam CT, the determination of the dose delivered to patients during complex CT exams becomes more difficult. Brenner in his 'Letter to the Editor' (Brenner 2005) questioned the use of the standard computed tomography dose index (CTDI) for CT quality assurance and dose optimization. More recently, Mori *et al* (2006) showed that the CTDI can no longer be used in multi-slice CT exams using scanners with a large detector size. The authors estimate the CT dose by using a conversion factor which is determined by a set of measurements with a 300 mm and a 100 mm long ionization chamber.

Another approach to estimate CT dose is using Monte Carlo (MC) methods (DeMarco *et al* 2005). Since the anatomy of individual patients can be included in the MC model, this approach is potentially superior to any other available method. However, in order to calculate the dose with a high accuracy, it is necessary to have an accurate Monte Carlo model of the CT scanner. The model has to include simulation of the x-ray tube, beam filters and shapers, and patient anatomy. In order to simulate image formation and image quality, the MC model has to be completed by the detector ring geometry. All the CT components have to be modelled with a high accuracy.

The aim of this work is to develop an accurate MC model of the CT x-ray tube. Spectral measurements on the central axis of the x-ray beam are performed and compared to spectra obtained by the MC model of the x-ray tube. Half-value layer (HVL) measurements are used in the Monte Carlo model for determination of inherent filtration of the x-ray tube.

For measurements of diagnostic x-ray spectra, semiconductor detectors are often used, such as high purity germanium (HP-Ge) (Nogueira *et al* 2004, Chen *et al* 1980, Bhat *et al* 1998) and compound semiconductors such as cadmium zinc telluride (CdZnTe) and cadmium telluride (CdTe). As opposed to HP-Ge detectors, detectors with a small thermoelectric cooling element (CdTe and CdZnTe) do not require a large liquid nitrogen cryogenic system which makes them very practical for measurements in radiological diagnostics. Whereas HP-Ge detectors are used for their excellent energy resolution, compound semiconductor detectors are used for their compactness. Miyajima (2003) showed that CdZnTe spectra are distorted due to charge trapping. He also demonstrated that correction for charge trapping of photon spectra measured by a CdTe detector is not necessary. Therefore, a novel generation CdTe spectrometer was used in our work.

It was shown in several works (Yaffe *et al* 1976, Matscheko and Ribberfors 1987, Matscheko and Carlsson 1989, Matscheko *et al* 1989, Maeda *et al* 2005) that due to the high photon fluence and consequent pile-up in the detector, spectral measurements of diagnostic x-ray tubes are not trivial. The high photon fluence can be decreased by using very small collimators (as small as 50 μm in diameter) and placing the detector several metres away from the focal spot which is, in the case of CT scanners, impossible.

The Compton scattering technique, introduced in radiological imaging by Yaffe *et al* (1976) and developed in several works by Matscheko and Ribberfors (1987), Matscheko and Carlsson (1989) and Matscheko *et al* (1989), is also very efficient in reducing the number of photons. These workers designed a device known as a Compton spectrometer that measures 90° scattered photons from a scattering object. They studied the effect of different scattering materials and geometries on the energy resolution of the whole system. More recently, Maeda *et al* (2005) measured diagnostic x-ray spectra using Compton scattering on a carbon scattering target. This geometry is rather simple and can easily be accommodated in a CT scanner. As far as we know, the technique has not yet been reported for use in CT scanners.

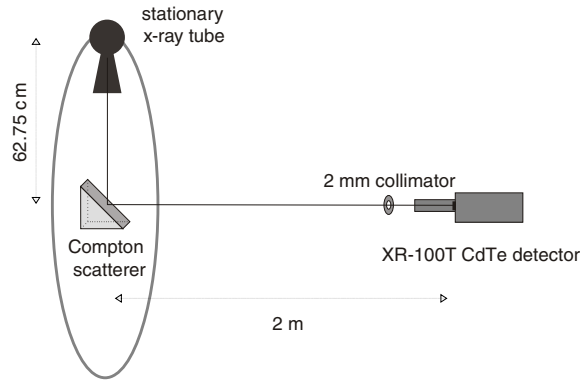

Figure 1. Compton scattering set-up for spectral measurements.

In this work, a MC model of a CT x-ray tube based on HVL measurements was created. We then compared MC simulated spectra to CT spectra measured by the Compton method using a high resolution CdTe detector and scattering on a carbon scatterer. The MC simulated spectra were also compared to spectra produced by the TASMIP (Boone and Seibert 1997) algorithm. TASMIP is a code that interpolates measured constant potential x-ray spectra published by Fewell *et al* (1981).

An accurate MC model of a CT x-ray tube is a first step towards developing a model of a whole CT scanner that will allow us to estimate the CT dose. It will also be a useful tool for understanding imaging processes and might be helpful in reducing scatter and CT artefacts, such as metal streaking artefacts.

2. Materials and methods

2.1. Spectral measurements

Spectral measurements of the x-ray tube (Rhino 6.5, DUNLEE, Illinois, USA) of our CT scanner (Picker PQ5000, Royal Philips Electronics, Eindhoven, the Netherlands) were performed with a high resolution Schottky CdTe spectrometer (XR-100T, AMPTEK Inc., Bedford, MA) in a Compton scatter set-up. The detector is a 3×3 mm^2 and 1 mm thick CdTe crystal with an energy resolution of 1.1% for ^{57}Co (122 keV). The detector operated at a bias voltage of 500 V. The energy calibration was done with the 31 keV peak of ^{133}Ba. The energy bin widths for the multichannel analyser were set to 0.5 keV.

The x-ray tube was in a stationary position, pointing downward, as shown in figure 1. A carbon scatterer (a $2 \times 2 \times 2$ cm^3 carbon block cut at 45°) was positioned at the isocentre of the gantry. A carbon scatterer was chosen because of its low atomic number with no characteristic x-rays above 0.3 keV. The spectrometer was placed on the couch at 2 m from the isocentre to minimize the range of scattering angles. In addition, a 2 mm diameter tungsten collimator was mounted on the detector in order to further reduce the scattering angle range and to prevent the scattered photons from interacting at the edge of the CdTe crystal.

2.1.1. Detector response. The measured spectra are distorted by the response of the detector. Therefore, they have to be corrected for photoelectric, coherent scattering and Compton scattering interactions that occur in the CdTe crystal. Seltzer (1981) introduced a procedure,

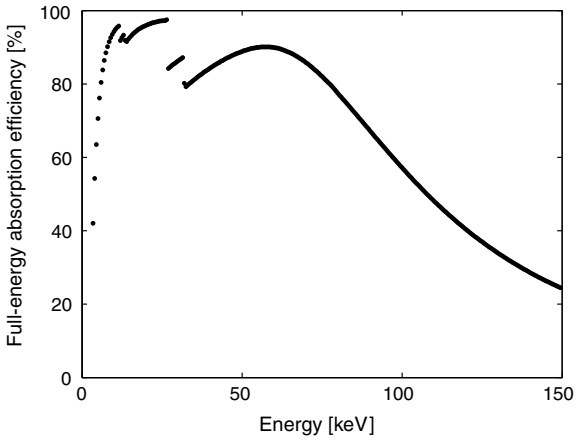

Figure 2. Full-energy absorption efficiency of a 1 mm thick CdTe detector calculated with the EGSnrc/DOSXYZnrc code.

described as a stripping method, that corrects for the detector response. The stripping method was later modified by Maeda *et al* (2005) to the following form:

$$N_t(E_0) = \frac{N_d(E_0) - \sum_{E=E_0+0.5}^{E_{\max}} R(E_0, E) N_t(E)}{R(E_0, E_0)}, \tag{1}$$

where $N_t(E_0)$ is the true number of photons with energy E_0 (in keV), $N_d(E_0)$ is the number of photons detected with E_0, $E_{\max}$ is the maximum energy in the detected spectrum, $R(E_0, E)$ is the monoenergetic response function, and $R(E_0, E_0)$ is the full-energy absorption peak efficiency. The monoenergetic response functions were obtained using Monte Carlo simulations in a modified version of the EGSnrc/DOSXYZnrc (Walters *et al* 2007) code. Monoenergetic beams (3.0 to 150 keV in 0.5 keV intervals) of 2 mm in diameter impinged on a $(3 \times 3 \times 1)$ mm^3 CdTe crystal and the monoenergetic response functions were determined by scoring the energy deposited in the crystal. The beryllium window (100 μm) and the two 200 nm metallic contacts (Pt on top and In on bottom) were also included in the geometry. Similarly to work by Miyajima (2003), the effects of carrier trapping and the dead layer of the crystal were not included in the response functions because they were shown to be insignificant in thin crystals operating at high voltages.

The full-energy absorption efficiency of the 1 mm thick CdTe spectrometer calculated from the response functions is presented in figure 2. It is in good agreement with the curve calculated with the LSCAT/EGS4 code presented by Miyajima (2003). The discontinuities are due to K-absorption edges of Cd and Te and L-absorption edges of Pt.

2.1.2. Reconstruction of primary spectra. The primary x-ray spectra were found by correcting the 90° scattered spectra for Compton scatter using an energy shift, the Klein–Nishina formula and deconvolution of the characteristic x-ray peaks. The attenuation in air due to the 2 m air gap between the scatterer and the spectrometer was also taken into account. The scatterer was removed and multiple-scatter radiation that was not due to the 90° Compton scattering on the carbon block was measured. The scatter from the CT gantry, the couch and the walls was found to be insignificant for our measurement.

The primary photons with energy $h\nu$ scattered at 90° were detected with energy $h\nu'$. The primary photon energy can be calculated from

$$h\nu = \frac{h\nu'}{1 - \frac{h\nu'}{m_e c^2}}, \tag{2}$$

where $m_e c^2$ is the rest mass of an electron.

The primary spectra $\phi_0(h\nu)$ are reconstructed from the intensities of the scattered spectra $\phi'(h\nu)$ by using the Klein–Nishina formula (Maeda *et al* 2005):

$$\phi_0(h\nu) = \phi'(h\nu) \Big/ \frac{1}{2}\left(\frac{1}{1+\alpha}\right)^2 \left(1 + \frac{\alpha^2}{1+\alpha}\right), \tag{3}$$

where $\alpha = h\nu/m_e c^2$.

The velocities of the scattering electrons in the carbon target cause a Doppler shift in the scattered photon energies (Ribberfors 1975) which results in broadening of the characteristic x-ray peaks. Matscheko and Ribberfors (1987) developed a deconvolution method that reconstructs the characteristic peaks $\phi_1(h\nu)$ from the primary photon spectrum $\phi_0(h\nu)$. The method was implemented in our work as the following, assuming a 90° scattering:

$$\phi_1(h\nu) = \phi_0(h\nu) - \frac{T}{3m_e c^2}\left(\frac{\nu}{\nu'}\right)^2 \left[\frac{d^2\phi_0(h\nu)}{d(h\nu)^2}[(h\nu)^2 + (h\nu')^2] + 2h\nu\left(\frac{d\phi_0(h\nu)}{d(h\nu)}\right)\right], \tag{4}$$

where T is a measure of the mean kinetic energy of the bound electrons in the scatterer which is 0.101 keV for carbon (Matscheko *et al* 1989). As pointed out by the authors, the deconvolution is strongly dependent on derivatives of $\phi_0(h\nu)$ and therefore should be used only in energy intervals that contain the characteristic x-ray peaks. Thus, the deconvolution of the spectrum was applied in the bins with energies between 57 keV and 61 keV (K_α tungsten lines) and in the bins with energies between 66 keV and 70 keV (K_β lines). The unfolded primary spectrum is then the combination of the primary spectrum $\phi_0(h\nu)$ calculated by equation (3) and the deconvolved spectrum $\phi_1(h\nu)$ at the position of the characteristic x-ray peaks.

2.2. Half-value layer measurements

The half-value layer (HVL_1) is the thickness of specified material (aluminium) that will reduce the air-kerma rate of a narrow beam of radiation to one-half its initial value (Ma *et al* 2001). The second HVL (HVL_2) is the additional thickness of the absorber that attenuates the air-kerma rate to 25% of its initial value. HVL is a beam quality specifier that together with tube voltage and total filtration is often used to characterize diagnostic x-ray spectra. It was used in our work to determine the inherent filtration of the x-ray tube with the MC model, as the manufacturer specifies only a nominal thickness.

HVL_1 and HVL_2 on the central axis were determined by attenuation measurements of a stationary x-ray tube using a Roos ionization chamber (PTW, Freiburg, Germany) and high purity 1 mm thick aluminium foils. The output of the x-ray tube was monitored by an Exradin A14 ionization chamber (Standard Imaging Inc., Middleton, WI).

2.3. MC simulation

The CT x-ray tube was modelled with the EGSnrc/BEAM (Rogers *et al* 1995) Monte Carlo code. The code includes an x-ray tube component module that was used for our simulation. The x-ray tube parameters were set according to the manufacturer's specifications.

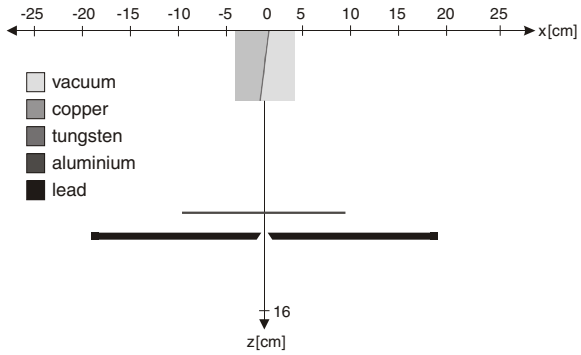

Figure 3. MC model of the CT x-ray tube.

2.3.1. CT specifications. The small (0.4 × 0.7) mm^2 and the large (0.6 × 1.3) mm^2 focal spots are produced by accelerated electrons striking a tungsten target. The x-ray tube offers high voltage potentials between 80 and 140 kV and tube currents between 30 mA to 300 mA. The anode has a 7° tilt and the anode heat is dissipated through a copper heat sink. The x-ray tube is evacuated. The inherent filtration due to the housing window is equivalent to a nominal thickness of 1.5 mm of aluminium according to the manufacturer's specifications. Additional 4.5 mm and 9.0 mm aluminium filtration is also available.

Head or body compensators can be used in order to account for non-uniform tissue thickness across the various exposed parts of the body and thus to achieve a more uniform beam intensity at the detector ring. Lead collimators define the field of view and slice thickness. The available slice thicknesses vary from 1 to 10 mm and the full and half field sizes are produced by a 38.4° and 19.2° fan beam, respectively.

2.3.2. The Monte Carlo model. The x-ray tube was modelled according to the specifications (figure 3). The lead collimator was set to produce the full field size and 1 mm slice thickness. The inherent filtration of the x-ray tube was initially set to 1.5 mm of aluminium. However, due to deposition of tungsten on the tube window caused by tube ageing (Nagel 1988), the inherent filtration increases with time. To account for tube ageing and attenuation of the beam as it passes through various structures such as the tube window, the inherent filtration was iteratively modified until good agreement with the HVL attenuation measurements was obtained. The simulated spectra were then compared to spectra measured with the CdTe detector.

All Monte Carlo simulations were run with 3.10^9 histories, the cut-off energies for electrons and photons were 20 and 10 keV, respectively. In order to obtain the correct number of photons in the characteristic x-ray peaks, the electron impact ionization process, which is by default off in the EGSnrc code, was on. Bound Compton scattering, Rayleigh scattering and atomic relaxations were also included in the simulations.

3. Results

3.1. Spectral measurements

Spectral measurements were performed for two tube voltages (100 and 140 kVp), and with and without the 9.0 mm aluminium filter. The spectral processing for the 140 kVp spectrum filtered by an additional 9.0 mm of aluminium is shown in figure 4.

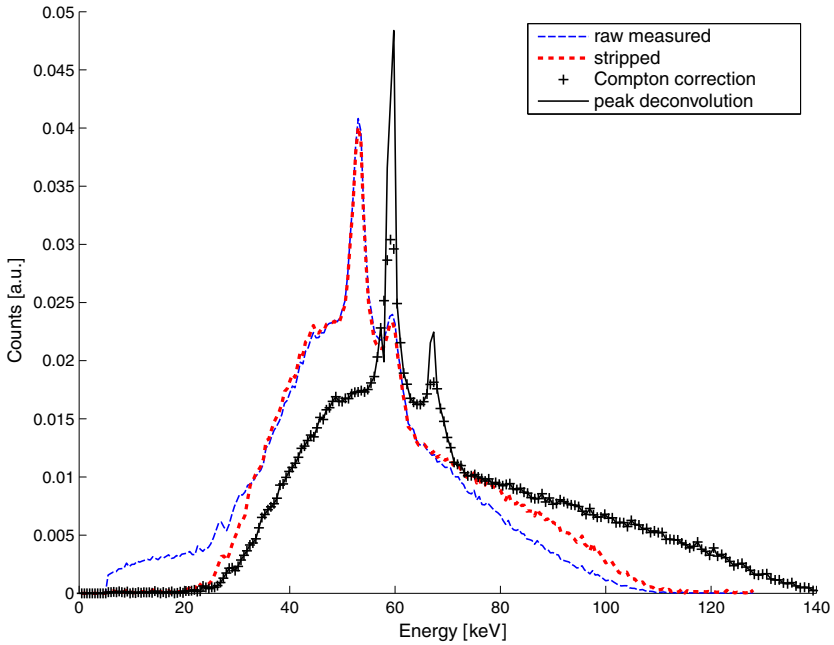

Figure 4. Spectral processing: raw measured spectrum (dashed line), stripped spectrum corrected for detector response (dotted line). Spectrum corrected for Compton scatter with broad characteristic x-ray peaks due to Doppler shift (crosses) and with deconvolved characteristic peaks (solid line).

The dashed line is the raw scattered spectrum acquired by the detector. The low-energy tail (1–20 keV) is produced entirely by the spectrometer. The raw spectrum is corrected for detector response by the stripping method (dotted line). Note that the low-energy tail produced by the detector disappeared. The crossed curve is created by applying the corrections based on the energy shift, the Klein–Nishina formula and the attenuation in air. Finally, the solid line corresponds to the primary x-ray tube spectrum. It is produced by deconvolution of the characteristic x-ray peaks of the crossed curve. The area under each curve is equal to unity.

The spectrum corrections were subsequently applied to all acquired spectra and thus primary spectra were obtained for 100 kVp and 140 kVp with and without a 9.0 mm aluminium filter.

3.2. HVL measurements

HVL measurements were carried out for 100 kV and 140 kV tube voltages with and without a 9.0 mm aluminium filter. HVL_1 and HVL_2 were iteratively determined on the basis of measured attenuation curves. The results are shown in table 1. HVL values were also iteratively calculated from the measured spectra, as done in the work by Verhaegen *et al* (1999). The percentage differences from HVL values calculated from the measured spectra are also listed in table 1. All differences between HVL values determined from attenuation curves and calculated from measured spectra are within 4.6%.

As can be seen in table 1, the HVL values for the beams with an additional 9 mm aluminium filtration determined by the attenuation measurement are consistently higher than

Table 1. HVL values (in mm of aluminium) and percentage differences (HVL_{PTW}-HVL_{CdTe})/HVL_{CdTe} as determined from attenuation measurements with a PTW chamber and as calculated from measured spectra with the CdTe detector. The values in the brackets are HVL values corrected for the PTW energy response.

		No additional filtration			Additional 9.0 mm Al		
		PTW (mm) Al	CdTe (mm) Al	$diff_{PTW\text{-}CdTe}$ (%)	PTW (mm) Al	CdTe (mm) Al	$diff_{PTW\text{-}CdTe}$ (%)
100 kVp	HVL_1	3.67	3.73	−1.6	6.64 (6.57)	6.40	3.8 (2.7)
	HVL_2	5.91	5.83	1.4	8.05 (7.93)	7.87	2.3 (0.8)
140 kVp	HVL_1	5.57	5.51	1.1	8.70 (8.60)	8.32	4.6 (3.4)
	HVL_2	7.84	7.95	−1.4	10.58 (10.27)	10.18	3.9 (0.9)

Table 2. HVL values (in mm of aluminium) and percentage differences (HVL_{MC} – HVL_{PTW})/HVL_{PTW} and (HVL_{MC}–HVL_{CdTe})/HVL_{CdTe} as measured with the PTW chamber, as calculated from MC simulated spectra and as calculated from measured spectra with the CdTe spectrometer.

		No additional filtration					Additional 9.0 mm Al		
		PTW (mm) Al	MC (mm) Al	$diff_{MC\text{-}PTW}$ (%)	CdTe (mm) Al	$diff_{MC\text{-}CdTe}$ (%)	CdTe (mm) Al	MC (mm) Al	$diff_{MC\text{-}CdTe}$ (%)
100 kVp	HVL_1	3.67	3.76	2.5	3.73	0.8	6.40	6.49	1.4
	HVL_2	5.91	5.76	−2.5	5.83	−1.2	7.87	7.80	−0.9
140 kVp	HVL_1	5.57	5.46	−2.0	5.51	−0.9	8.32	8.47	1.8
	HVL_2	7.84	8.03	2.4	7.95	1.0	10.18	10.15	−0.3

the values calculated from the measured spectra. This can be explained by the non-flat energy response of the ionization chamber. According to the NRC Calibration Report of the chamber, the reading for a 9.5 mm aluminium HVL beam is by 4% higher than the reading for a 3.0 mm HVL beam. When a correction for this was performed, assuming a linear energy response of the ionization chamber in the HVL range (6.49–11.07) mm aluminium, the values in the brackets given in table 1 were obtained. This leads to smaller differences with the HVL values derived from the CdTe spectrometer, as indicated in the last column.

3.3. MC simulations

In order to complete the MC x-ray tube model as specified by the manufacturer, the inherent filtration had to be determined. First, it was set to 1.5 mm of aluminium and iteratively altered until good agreement with HVL attenuation measurements for beams with no additional filtration was found. This process resulted in the value of 1.90 mm of aluminium. As can be seen from the third column of table 2 ($diff_{MC\text{-}PTW}$), 1.90 mm of aluminium leads to HVL differences smaller than 2.5%. The MC calculated spectra are also compared to the CdTe calculated spectra in table 2. The HVL values for beams with no additional filtration show very good agreement, the differences are within 1.2%. The HVL values for beams filtered with additional 9 mm of aluminium are within 1.8%.

Once the inherent filtration of the x-ray tube is established, Monte Carlo simulated spectra can be compared to the measured spectra. The results are shown in figure 5. Good agreement

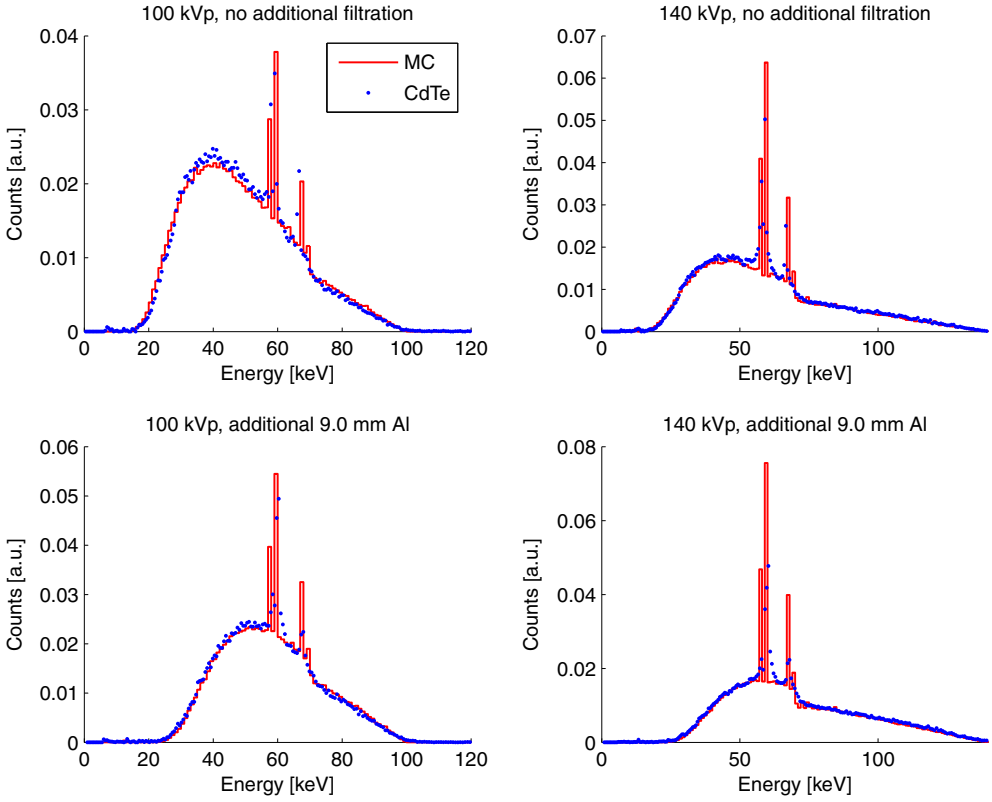

Figure 5. Comparison of spectra measured with the CdTe detector (dotted curve) and simulated with Monte Carlo (full line). The area under each curve equals unity.

between measurements and MC simulations was found. The largest discrepancies are observed for the non-filtered 100 kVp spectrum in the area where Bremsstrahlung radiation has its peak which can be partially explained by noise in the CdTe measurements. The tungsten K-lines measured by the detector always have a lower intensity than the K-lines calculated by MC. This is primarily due to the energy resolution of the spectrometer that was measured to be 1.42 keV at 122 keV. However, the differences in the total net areas of the characteristic peaks from the spectrometer measurements and MC simulations are within 20% which has a negligible effect on dose calculations.

MC simulated spectra were also compared to spectra calculated by the TASMIP program (Boone and Seibert 1997). Figure 6 shows the comparison for the 100 kVp spectrum with added filtration and for the 140 kVp spectrum without filtration. Similarly to the comparison of MC simulated spectra and measured spectra with the CdTe detector, the intensities of the TASMIP characteristic peaks are smaller than the intensities predicted by MC. This is due to the calculation resolution of TASMIP which is 2 keV. In general, a very good agreement in the determination of spectra between TASMIP and MC was found.

In conclusion, for purposes where only diagnostic x-ray spectra without spatial information are needed, the TASMIP program can be conveniently benefited from. However, the TASMIP program cannot be used for Monte Carlo simulation of a CT scanner where high precision on photon fluence distribution or scatter distribution is required. The information

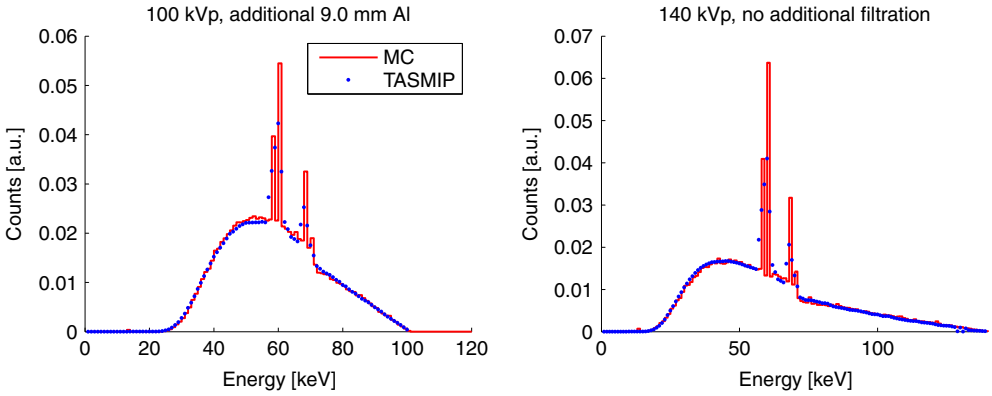

Figure 6. MC simulated spectra (full line) compared to TASMIP spectra (dotted curve).

on photon positions and directions can be calculated only by full MC simulation of the entire CT scanner geometry, including the x-ray tube.

4. Conclusions

A Monte Carlo model of a CT x-ray tube was validated by measurements of x-ray beams produced by two different tube voltages and filtrations. HVL_1 and HVL_2 for beams without additional filtration calculated from the MC modelled spectra and determined from attenuation measurements differ by less than 2.5%. The differences between HVL_1 and HVL_2 calculated from the MC modelled spectra and determined from spectral measurements with a CdTe detector are within 1.8%. The MC modelled spectra were directly compared to spectra measured by the CdTe detector and to spectra calculated by the TASMIP program and good agreement was found.

We have created a Monte Carlo model of a CT x-ray tube. The model can now be completed by the compensator and the detector ring geometry and the dose delivered to the patients can be calculated by the Monte Carlo method. The model will also be helpful in understanding CT imaging processes and the creation of CT artefacts.

Acknowledgments

We would like to acknowledge Hatchig Ibisoglu from Philips for the Picker PQ5000 specifications and Dr Wamied Abdel-Rahman for valuable discussion regarding Compton scatter. The CdTe detector was acquired with a grant from the Research Institute of the McGill University Health Center. The work has been supported by grant no. 206358 from the Natural Science and Engineering Research Council of Canada (NSERC). FV is a Research Scientist supported by the Fonds de la Recherche en Santé du Québec (FRSQ).

References

Bhat M, Pattison J, Bibbo G and Caon M 1998 Diagnostic x-ray spectra: a comparison of spectra generated by different computational methods with a measured spectrum *Med. Phys.* **25** 114–20

Boone J M and Seibert J A 1997 An accurate method for computer-generating tungsten anode x-ray spectra from 30 to 140 kV *Med. Phys.* **24** 1661–70

Brenner J D 2005 Is it time to retire the CTDI for CT quality assurance and dose optimization? *Med. Phys.* **32** 3225–6

Chen C S, Doi K, Vyborny C, Chan H-P and Holje G 1980 Monte Carlo simulation studies of detectors used in the measurement of diagnostic x-ray spectra *Med. Phys.* **7** 627–35

DeMarco J J, Cagnon C H, Cody D D, Stevens D M, McCollough C H, O'Daniel J and McNitt-Gray M F 2005 A Monte Carlo based method to estimate radiation dose from multidetector CT (MDCT): cylindrical and antromorphic phantoms *Phys. Med. Biol.* **50** 3989–4004

Fewell T R, Shuping R E and Healy K E 1981 Handbook of Computed Tomography X-ray Spectra 81-8162 (US Government Printing Office, Washington, DC: HHS Publication (FDA)

Ma C-M, Coffey C W, DaWerd L A, Liu C, Nath R, Seltzer S M and Seuntjens J P 2001 AAPM protocol for 40–300 kV x-ray beam dosimetry in radiotherapy and radiology *Med. Phys.* **28** 868–93

Maeda K, Matsumoto M and Taniguchi A 2005 Compton-scattering measurement of diagnostic x-ray spectrum using high-resolution Schottky CdTe detector *Med. Phys.* **32** 1542–7

Matscheko G and Carlsson G A 1989 Compton spectroscopy in the diagnostic x-ray energy range: I. Spectrometer design *Phys. Med. Biol.* **34** 185–97

Matscheko G, Carlsson G A and Ribberfors R 1989 Compton spectroscopy in the diagnostic x-ray energy range: II. Effects of scattering material and energy resolution *Phys. Med. Biol.* **34** 199–208

Matscheko G and Ribberfors R 1987 A Compton scattering spectrometer for determining x-ray photon spectra *Phys. Med. Biol* **32** 577–94

Miyajima S 2003 Thin CdTe detector in diagnostic x-ray spectroscopy *Med. Phys.* **30** 771–7

Mori S, Nishizawa K, Ohno M and Endo M 2006 Conversion factor for CT dosimetry to assess patient dose using a 256-slice CT scanner *Br. J. Radiol.* **79** 888–92

Nagel H D 1988 Limitations in the determination of total filtration of x-ray tube assemblies *Phys. Med. Biol.* **33** 271–89

Nogueira M S, Mota H C and Campos L L 2004 (HP)Ge measurement of spectra for diagnostic x-ray beams *Radiat. Prot. Dosim.* **111** 105–10

Ribberfors R 1975 Relationship of the relativistic Compton cross section to the momentum distribution of bound electron states *Phys. Rev.* B **12** 2067–74

Rehani M M, Bongartz G, Golding S J, Gordon L, Kalender W, Murakami T, Shrimpton P, Albrecht R and Wei K 2001 *Annals of the ICRP Report 87* vol 30/4

Rogers D W O, Faddegon B A, Ding G X, Ma C-M, We J and Mackie T R 1995 BEAM: a Monte Carlo code to simulate radiotherapy treatment units *Med. Phys.* **22** 503–24

Seltzer S M 1981 Calculated response of intrinsic germanium detectors to narrow beams of photons with energies up to ∼300 keV *Nucl. Instrum. Methods* **188** 133–51

Verhaegen F, Nahum A E, Van de Putte S and Namito Y 1999 Monte Carlo modelling of radiotherapy kV x-ray units *Phys. Med. Biol* **44** 1767–89

Walters B R B, Kawrakow I and Rogers DWO 2007 *DOSXYZnrc Users Manual N R CC Report* No. PIRS 794revB

Yaffe M, Taylor K W and Johns H E 1976 Spectroscopy of diagnostic x rays by a Compton-scatter method *Med. Phys.* **3** 328–34